CERN-TH/98-336
hep-ph/9811434

Radiative corrections to W-pair production in e^+e^- annihilation*

Stefan Dittmaier

Theory Division, CERN
CH-1211 Geneva 23, Switzerland

Abstract:
The status of precision calculations for the processes $e^+e^- \to WW \to 4$ fermions is reviewed, paying particular attention to questions of gauge invariance and recent progress concerning photonic radiative corrections.

CERN-TH/98-336
November 1998

*Contribution to the proceedings of *IVth International Symposium on Radiative Corrections, RADCOR 98*, 8–12 September 1998, Barcelona, Spain.

RADIATIVE CORRECTIONS TO W-PAIR PRODUCTION IN e^+e^- ANNIHILATION

STEFAN DITTMAIER

CERN, Theory Division, CH-1211 Geneva 23, Switzerland
E-mail: Stefan.Dittmaier@cern.ch

The status of precision calculations for the processes $e^+e^- \to WW \to 4$ fermions is reviewed, paying particular attention to questions of gauge invariance and recent progress concerning photonic radiative corrections.

1 Introduction

At present, the most stringent tests of our understanding of the electroweak interaction is obtained by confronting theoretical predictions with the experimental precision data on the various Z-boson resonance observables provided by LEP1 and the SLC, the Fermi constant G_μ, the effective electromagnetic coupling $\alpha(M_Z^2)$, and the masses M_W and m_t of the W boson and the top quark. The agreement between the Standard-Model (SM) predictions and those experimental results, which is at the impressive level of a few per mille, can be viewed as perfect (see Ref. [1] and references therein). Despite this success, two cornerstones of the electroweak SM still await direct empirical confirmation: the Higgs mechanism for the mass generation and the detailed structure of the gauge-boson self-interactions. The investigation of W-pair production in e^+e^- annihilation, as observed at LEP2 and future e^+e^- colliders, yields important contributions to both aspects.

The experimental analysis of the reaction $e^+e^- \to W^+W^-$ allows for a precise determination of M_W. In the first half of 1998, the W-mass measurement at LEP2 [2] already reached a precision of 90 MeV. At LEP2 a final error of 30–40 MeV [4] is aimed at, which could be further reduced to about 15 MeV by observing W pairs at a future e^+e^- linear collider [5]. Such an improved knowledge of M_W will strengthen the indirect constraints on the mass M_H of the SM Higgs boson, which are obtained by fitting the SM parameters to the electroweak precision data. In view of gauge-boson self-interactions, the process $e^+e^- \to W^+W^-$ yields more direct information, since the non-Abelian γWW and ZWW couplings enter the perturbative predictions already in lowest order. It is expected that LEP2 [6] will test these triple gauge-boson couplings (TGCs) at the level of 10% with respect to the SM coupling strength, and that

a future linear collider [5] can even exceed the per-cent level.

The desired information on the properties of the W boson is extracted from the cross section and the relevant angular and invariant-mass distributions for the process $\mathrm{e^+e^-} \to \mathrm{W^+W^-}$. More precisely, the W-boson mass is determined [4] by inspecting the total cross section near threshold, where it is most sensitive to M_W, and, sufficiently above threshold, by reconstructing the invariant mass of the W boson from its decay products. In the LEP2 energy range, restrictive bounds on TGCs [6] can only be obtained by considering various angular distributions, such as the one for the W-production angle. For higher energies, also the total cross section becomes more and more sensitive to TGCs.

The described experimental aims require the knowledge of the SM predictions for the mentioned observables to a high precision. For LEP2, the cross section of W-pair production should be known within $\sim 0.5\%$ [7]; future linear colliders with higher luminosity and energy set similar requirements. The theoretical precision for the invariant-mass distribution of the W bosons should, of course, exceed the expected experimental accuray given above. To achieve this level of precision in predictions is a highly non-trivial task, since the actually relevant reaction is the four-fermion process $\mathrm{e^+e^-} \to \mathrm{WW} \to 4f$, in which the unstable W bosons appear as resonances. The issue of gauge invariance requires particular attention, and the necessary inclusion of radiative corrections is not straightforward. In this article, these sources of complications and their consequences for actual calculations are discussed, and special emphasis is laid on recent developments. More details can be found in other review articles [7–10] and references therein.

2 The issue of gauge invariance

2.1 Finite gauge-boson widths and lowest-order predictions

At and beyond the per-cent accuracy, gauge-boson resonances cannot be treated as on-shell states in lowest-order calculations, since the impact of a finite decay width Γ_V for a gauge boson V of mass M_V can be roughly estimated to $\Gamma_\mathrm{V}/M_\mathrm{V}$, which is, for instance, $\sim 3\%$ for the W boson. Therefore, the full set of tree-level diagrams for a given fermionic final state has to be taken into account. For $\mathrm{e^+e^-} \to \mathrm{WW} \to 4f$ this includes graphs with two resonant W-boson lines ("signal diagrams") and graphs with one or no W resonance ("background diagrams"), leading to the following structure of the amplitude [7, 8, 11]:

$$\mathcal{M} = \underbrace{\frac{R_{+-}(k_+^2,k_-^2)}{(k_+^2-M_\mathrm{W}^2)(k_-^2-M_\mathrm{W}^2)}}_{\text{doubly-resonant}} + \underbrace{\frac{R_+(k_+^2,k_-^2)}{k_+^2-M_\mathrm{W}^2} + \frac{R_-(k_+^2,k_-^2)}{k_-^2-M_\mathrm{W}^2}}_{\text{singly-resonant}} + \underbrace{N(k_+^2,k_-^2)}_{\text{non-resonant}} . \tag{1}$$

Gauge invariance implies that $\mathcal{M}$ is independent of the gauge fixing used for calculating Feynman graphs (gauge-parameter independence), and that gauge cancellations between different contributions to $\mathcal{M}$ take place. These gauge cancellations are ruled by Ward identities (see e.g. Refs. [9, 13, 14]), and their violation can completely destroy the consistency of predictions [12–14].

For a physical description of the W resonances, the finite W decay width has to be introduced in the resonance poles. However, since only the sum in (1), but not the single contributions to $\mathcal{M}$, possesses the gauge-invariance properties, the simple replacement

$$\left[k^2 - M_{\mathrm{V}}^2\right]^{-1} \quad \to \quad \left[k^2 - M_{\mathrm{V}}^2 + \mathrm{i}M_{\mathrm{V}}\Gamma_{\mathrm{V}}(k^2)\right]^{-1} \tag{2}$$

in general violates gauge invariance. We describe in more detail some methods (see Refs. [7, 14–16] and references therein) for introducing finite gauge-boson widths in lowest-order amplitudes.

(i) The *fixed-width scheme* is nothing but the naive replacement (2) for all gauge-boson propagators where $\Gamma_{\mathrm{V}}(k^2)$ is the (constant) on-shell width Γ_{V}. In general, gauge dependences are introcuded, and the Ward identities are violated. For $\mathrm{e}^+\mathrm{e}^- \to 4f$, electromagnetic gauge invariance is maintained, and the SU(2)-violating effects are suppressed by the factor $\Gamma_{\mathrm{W}}M_{\mathrm{W}}/s$ in the high-energy limit [14].

(ii) The *running-width scheme* differs from the constant-width scheme only in the form of the function $\Gamma_{\mathrm{V}}(k^2)$ in (2), which is now chosen as $\Gamma_{\mathrm{V}}(k^2) = \Gamma_{\mathrm{V}} \times \theta(k^2)k^2/M_{\mathrm{V}}^2$. Although the running width seems to describe the propagator in a more realistic way at first sight, for $\mathrm{e}^+\mathrm{e}^- \to 4f$ not even electromagnetic gauge invariance is retained anymore [14].

(iii) The *complex-mass scheme* [16][a] demands the consistent replacement $M_{\mathrm{V}}^2 \to M_{\mathrm{V}}^2 - \mathrm{i}M_{\mathrm{V}}\Gamma_{\mathrm{V}}$ for the gauge-boson masses whenever a gauge-boson mass appears. In particular, this leads to the complex weak mixing angle defined by

$$c_{\mathrm{w}}^2 = 1 - s_{\mathrm{w}}^2 = \frac{M_{\mathrm{W}}^2 - \mathrm{i}M_{\mathrm{W}}\Gamma_{\mathrm{W}}}{M_{\mathrm{Z}}^2 - \mathrm{i}M_{\mathrm{Z}}\Gamma_{\mathrm{Z}}}, \tag{3}$$

i.e. coupling constants become complex-valued. As long as tree-level amplitudes are parametrized by a minimal set of input parameters, algebraic relations between Feynman diagrams remain unchanged so that gauge-parameter dependences still cancel, and Ward identities still hold.

[a] Aspects of such a scheme have already been discussed in Ref. [17] for the description of the Z-boson resonance in $\mathrm{e}^+\mathrm{e}^- \to \mathrm{Z} \to f\bar{f}$.

$\sqrt{s}$/ GeV	200	500	1000	2000
Fixed width	712.8(2)	237.3(1)	60.34(4)	13.97(1)
Running width	712.7(2)	238.7(1)	65.74(4)	34.40(2)
Complex mass	712.4(2)	237.1(1)	60.31(4)	13.97(1)

Table 1: CC10 cross section in fb for various finite-width schemes (based on the results of Ref. [16]).

$\sqrt{s}$/ GeV	200	500	1000	2000
Fixed width	673.08(4)	224.05(3)	56.90(1)	13.19(1)
Running width	672.96(3)	225.45(3)	62.17(1)	33.06(1)
Full fermion loops	683.7(1)	227.9(2)	58.0(1)	13.57(4)
Imag. fermion loops	673.1(1)	224.5(7)	56.8(1)	13.18(4)

Table 2: CC10 cross section in fb for various finite-width schemes (taken from Ref. [14]). The two versions for the fermion-loop scheme (numbers generated by *WTO* [18]) differ by the real parts of the fermion loops, which are included in the upper row but not in the lower.

Despite the nice features of this scheme, it should be used with care, as its full consistency is not yet clarified.

(iv) The *fermion-loop scheme* [14] goes beyond a pure tree-level calculation by including and consistently Dyson-summing all closed fermion loops in $\mathcal{O}(\alpha)$. This procedure introduces the running tree-level width in gauge-boson propagators via the imaginary parts of the fermion loops. Ward identities are not violated, since the fermion-loop (as well as the tree-level) contributions to vertex functions obey the simple linear (also called "naive") Ward identities that are related to the original gauge invariance rather than to the more involved BRS invariance of the quantized theory. Owing to the linearity of the crucial Ward identities for the vertex functions, the fermion-loop scheme works both with the full fermion loops and with the restriction to their imaginary parts. Simplified versions of the scheme have been introduced in Ref. [13].

Tables 1 and 2 contain some results[b] on the cross section for the "CC10 process" $e^+e^- \to u\bar{d}\mu^-\bar{\nu}_\mu$ for the different finite-width schemes. The energies are typical of LEP2 and future linear colliders, and the phase space is restricted by the "canonical LEP2 cuts" of Ref. [19]. In the high-energy limit, SU(2) gauge invariance implies delicate cancellations between different diagrams. The

[b] The input data for the two tables are different, because the complex-mass scheme [16] requires a minimal set of input parameters with relation (3), while s_W was deduced from the Fermi constant in the evaluation of the fermion-loop scheme in Ref. [14].

complex-mass and the fermion-loop schemes fully respect these cancellations, since the underlying Ward identities hold, resulting in reliable predictions for high energies. Both the fixed and running width break SU(2) invariance so that the gauge cancellations are disturbed. While the gauge-invariance-breaking terms grow like s/M_{W}^2 for the running width scheme, leading to totally wrong results already in the TeV range, those terms are suppressed for the fixed-width scheme (see above), still yielding reasonable results for high energies.

2.2 Looking beyond lowest order

Among the methods to introduce finite gauge-boson widths in tree-level amplitudes, the field-theoretically most convincing one is the fermion-loop scheme, since the widths are consistently generated by the inclusion of the relevant higher-order effects. It is therefore natural to worry about a generalization of this scheme when considering higher-order corrections to amplitudes. There are basically two sources of limitation for the fermion-loop scheme.

Firstly, the fermion-loop scheme is not applicable in the presence of resonant particles that do not exclusively decay into fermions. For such particles, parts of the decay width are contained in bosonic corrections. The Dyson summation of fermionic *and* bosonic $\mathcal{O}(\alpha)$ corrections leads to inconsistencies in the usual field-theoretical approach, i.e. Ward identities are broken in general. This is due to the fact that the bosonic $\mathcal{O}(\alpha)$ contributions to vertex functions do not obey the "naive Ward identities". The problem is circumvented by employing the background-field formalism [20], in which these naive identities are valid. This implies [21] that a consistent Dyson summation of fermionic and bosonic corrections to any order in α does not disturb Ward identities. Therefore, the background-field approach provides a natural generalization of the fermion-loop scheme. We recall that any resummation formalism goes beyond a strict order-by-order calculation and necessarily involves ambiguities in relative order α^n if not all n-loop diagrams are included. This kind of scheme dependence, which in particular concerns gauge dependences, is only resolved by successively calculating the missing orders.

Secondly, the consistent resummation of all $\mathcal{O}(\alpha)$ loop corrections does not automatically lead to $\mathcal{O}(\alpha)$ precision in the predictions if resonances are involved. The imaginary parts of one-loop self-energies generate only tree-level decay widths so that directly on resonance one order in α is lost. To obtain also full $\mathcal{O}(\alpha)$ precision in these cases, the imaginary parts of the two-loop self-energies are required. However, how and whether this two-loop contribution can be included in a practical way without violating Ward identities is still an open problem. Taking the imaginary parts of all two-loop contributions solves the problem in principle, at least for the background-field approach, but this

θ range	$\sqrt{s}$/ GeV	161	175	200	500	1000	2000
$0°<\theta<180°$	$(\delta_{\rm IBA}-\delta)/\%$	1.5	1.3	1.5	3.7	6.0	9.3
$10°<\theta<170°$		1.5	1.3	1.5	4.7	11	22

Table 3: Size of "non-leading" corrections to on-shell W-pair production ($\delta_{\rm IBA}$ and δ include only soft-photon emission).

is certainly impractical.

3 Electroweak radiative corrections

3.1 Relevance of electroweak corrections

Present-day Monte Carlo generators for off-shell W-pair production (see e.g. Ref. [19]) typically include only universal electroweak $\mathcal{O}(\alpha)$ corrections[c], such as the running of the electromagnetic coupling, $\alpha(q^2)$, leading corrections entering via the ρ-parameter, the Coulomb singularity [23], which is important near threshold, and mass-singular logarithms $\alpha\ln(m_{\rm e}^2/Q^2)$ from initial-state radiation. In leading order, the scale Q^2 is not determined and has to be set to a typical scale for the process; for the following we take $Q^2=s$.

Since the full $\mathcal{O}(\alpha)$ correction is not known for off-shell W pairs, the size of the neglected $\mathcal{O}(\alpha)$ contributions is estimated by inspecting on-shell W-pair production, for which the exact $\mathcal{O}(\alpha)$ correction and the leading contributions were given in Refs. [24] and [25], respectively. Table 3 shows the difference between an "improved Born approximation" $\delta_{\rm IBA}$, which is based on the above-mentioned universal corrections, and the corresponding full $\mathcal{O}(\alpha)$ correction δ to the Born cross-section integrated over the W-production angle θ for some centre-of-mass energies $\sqrt{s}$. More details and results can be found in Refs. [7, 9]. The quantity $\delta_{\rm IBA}-\delta$ corresponds to the neglected non-leading corrections and amounts to $\sim$ 1–2% for LEP2 energies, but to $\sim$ 10–20% in the TeV range. Thus, in view of the needed 0.5% level of accuracy for LEP2 and all the more for energies of future linear colliders, the inclusion of non-leading corrections is indispensable. The large contributions in $\delta_{\rm IBA}-\delta$ at high energies are due to terms such as $\alpha\ln^2(s/M_{\rm W}^2)$, which arise from vertex and box corrections and can be read off from the high-energy expansion [26] of the virtual and soft-photonic $\mathcal{O}(\alpha)$ corrections.

A first step of including electroweak corrections in an event generator was made by Jadach et al. [27], who took into account the full virtual [24] and real-photonic [28] $\mathcal{O}(\alpha)$ corrections to the on-shell W-pair production process, but neglected the corrections associated with the decay of the W bosons. In order

[c] The QCD corrections for hadronic final states are discussed in Ref. [22].

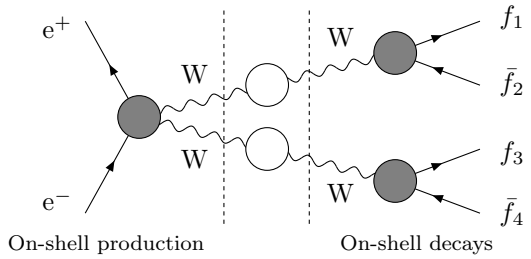

Figure 1: Diagrammatic structure of factorizable corrections to $e^+e^- \to WW \to 4f$.

to gain an accuracy of 0.5–1% for realistic observables, it is, however, necessary to develop a more complete strategy for the full process $e^+e^- \to WW \to 4f$.

3.2 Double-pole approximation

Fortunately, the full off-shell calculation for the process $e^+e^- \to WW \to 4f$ in $\mathcal{O}(\alpha)$ is not needed for most applications. Sufficiently above the W-pair threshold a good approximation should be obtained by taking into account only the doubly-resonant part of the amplitude (1), leading to an error of the order of $\alpha\Gamma_W/(\pi M_W) \lesssim 0.1\%$. In such a "pole scheme" calculation [11, 29], also called double-pole approximation (DPA), the numerator $R_{+-}(k_+^2, k_-^2)$ has to be replaced by the gauge-independent residue $R_{+-}(M_W^2, M_W^2)$.

Doubly-resonant corrections to $e^+e^- \to WW \to 4f$ can be classified into two types [7, 8, 11]: factorizable and non-factorizable corrections. The former are those that correspond either to W-pair production or to W decay. They are represented by the schematic diagram of Fig. 1, in which the shaded blobs contain all one-loop corrections to the production and decay processes, and the open blobs include the corrections to the W propagators. The remaining corrections are called non-factorizable, since they do not contain the product of two independent Breit–Wigner-type resonances for the W bosons, i.e. the production and decay subprocesses are not independent in this case. Non-factorizable corrections include all diagrams involving particle exchange between these subprocesses. Simple power-counting arguments reveal that such diagrams only lead to doubly-resonant contributions if the exchanged particle is a photon with energy $E_\gamma \lesssim \Gamma_W$; all other non-factorizable diagrams are negligible in DPA. Two relevant diagrams are shown in Fig. 2, where the full blobs represent tree-level subgraphs. We note that diagrams involving photon exchange between the W bosons (see Fig. 3) contribute both to factorizable and non-factorizable corrections; otherwise the splitting into those parts is not gauge-invariant. The non-factorizable corrections to $e^+e^- \to WW \to 4f$ will be discussed in Sect. 3.5 in more detail.

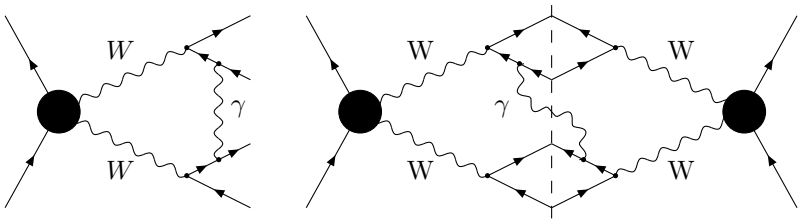

Figure 2: Examples of virtual and real non-factorizable corrections to $e^+e^- \to WW \to 4f$.

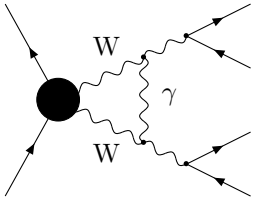

Figure 3: Feynman graph contributing to both factorizable and non-factorizable corrections.

The factorizable corrections consist of contributions from virtual corrections and real-photon bremsstrahlung. The known results on the virtual corrections to the pair production [24] and the decay [30] of on-shell W bosons can be used as building blocks for the DPA. Because of the complex structure of the virtual corrections to the production process, simple approximations are desirable. In the LEP2 energy range, approximations [25, 31] that are mainly based on universal corrections describe the total cross section within $\sim 0.5\%$ and the angular distribution within 1–2% relative to the lowest order. For energies above 500 GeV, a consistent high-energy expansion [26, 32] reaches per-cent accuracy whenever the cross section is sizeable. However, a satisfying, simple approximation for all relevant energies is not available.

The formulation of a consistent DPA for the bremsstrahlung corrections is non-trivial. The main complication originates from the emission of photons from the resonant W bosons. A radiating W boson involves two propagators whose momenta differ by the momentum of the emitted photon. If the photon momentum is large ($E_\gamma \gg \Gamma_W$), the resonances of these two propagators are well separated in phase space, and their contributions can be associated with photon radiation from exactly one of the production or decay subprocesses. For soft photons ($E_\gamma \ll \Gamma_W$) a similar splitting is possible. However, for $E_\gamma \sim \Gamma_W$ the two resonance factors for the radiating W boson overlap so that a simple decomposition into contributions associated with the subprocesses is not obvious.

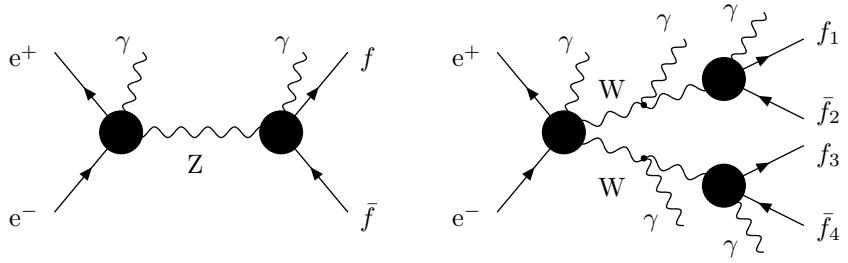

Figure 4: Illustration of photon radiation in $e^+e^- \to Z \to f\bar{f}$ and $e^+e^- \to WW \to 4f$.

A full application of the DPA to $e^+e^- \to WW \to 4f$ has not yet been presented in the literature, but first preliminary results have been shown by Berends [33] at this conference.

3.3 Photon radiation and W line shape

A thorough description of real-photon emission is of particular importance for the realistic prediction of the W line shape, which is the basic observable for the reconstruction of the W-boson mass from the W-decay products. This fact can be easily understood by comparing the impact of photon radiation on the line shape of the W boson with the one of the Z boson, observed in $e^+e^- \to Z \to f\bar{f}$ at LEP1 and the SLC (see Fig. 4).

The Z line shape is defined as a function of s, which is fully determined by the initial state, by the cross section $\sigma(s)$. Photon radiation from the initial state effectively reduces the value of s that is "seen" by the Z boson so that $\sigma(s)$ also receives resonant contributions for $s > M_Z^2$, induced by this *radiative return* to the Z resonance and known as *radiative tail*. Final-state radiation is not enhanced by such kinematical effects, thus yielding moderate corrections.

The W line shape is reconstructed from the kinematical variables in the final state. More precisely, it is defined by the distributions $d\sigma/dM_\pm^2$, where $M_\pm^2$ are the reconstructed invariant masses of the $W^\pm$ bosons. We now consider the fermion pair $f_1(k_1)\bar{f}_2(k_2)$ produced by a nearly resonant W boson with momentum k_+, i.e. $k_+^2 \sim M_W^2$. In this case, photon radiation from the final state decreases the invariant mass of this fermion pair, i.e. $(k_1+k_2)^2 < k_+^2 = (k_1+k_2+k_\gamma)^2$, while initial-state radiation leads to $(k_1+k_2)^2 = k_+^2 < (k_1+k_2+k_\gamma)^2$. Thus, a consistent identification of $M_+^2 = (k_1+k_2)^2$ also leads to a radiative tail, but now induced by final-state radiation and for $M_+^2 < M_W^2$. However, such an identification is experimentally not possible for almost all cases,[d] since nearly collinear and soft photons in the final state cannot be fully

[d] Semi-leptonic final states with a muon may be an exception, where $(k_\mu + k_{\nu_\mu})^2$ could

separated from the outgoing fermions (except for muons). A realistic definition of $M_{\pm}^2$ necessarily depends on the details of the experimental treatment of photons in the final state, underlining the importance of a careful investigation of the W line shape in the presence of photon radiation.

The line-shape distortion by photon emission was discussed in Ref. [34] also quantitatively. Based on an exact treatment of the Z boson line shape in $\nu_\mu\bar{\nu}_\mu \to \mathrm{ZZ} \to \mathrm{e}^-\mathrm{e}^+\nu_\tau\bar{\nu}_\tau$, an estimate for the process $\mathrm{e}^+\mathrm{e}^- \to \mathrm{WW} \to 4f$ could be obtained by an analysis in leading-logarithmic accuracy. Assuming the idealized definition $M_+^2 = (k_1 + k_2)^2$, the authors of Ref. [34] find shifts in the peak position of $\mathrm{d}\sigma/\mathrm{d}M_+^2$ of several times $-10\,\mathrm{MeV}$ and peak reduction factors in the range 0.95–0.75. The maximal effect was obtained for $\mathrm{W}^+ \to \mathrm{e}^+\nu_\mathrm{e}$, leading to $\Delta M_+ \sim -45\,\mathrm{MeV}$. Note, however, that these large corrections are formally due to mass-singular logarithms such as $\alpha\ln(m_\mathrm{e}/M_\mathrm{W})$, which are effectively replaced by logarithms of a minimum opening angle for collinear photon emission in more realistic definitions of M_+^2. Therefore, it is expected that the corrections are somewhat weakened in realistic situations.

3.4 The process $\mathrm{e}^+\mathrm{e}^- \to 4f + \gamma$

The process $\mathrm{e}^+\mathrm{e}^- \to 4f + \gamma$ does not only yield important corrections to $\mathrm{e}^+\mathrm{e}^- \to 4f$, as explained above, it is also interesting in its own right, since it involves both triple and quartic gauge-boson couplings. Most of the existing work on hard-photon radiation in W-pair production is based on the approximation of stable W bosons (see Ref. [28] and references in Refs. [7, 16]). A first step of including the off-shellness of W bosons in $\mathrm{e}^+\mathrm{e}^- \to \mathrm{WW} \to 4f + \gamma$ was done in Ref. [35], where only photon emission from the signal diagrams of W-pair production was taken into account. However, it is desirable to have a full lowest-order calculation for $\mathrm{e}^+\mathrm{e}^- \to 4f + \gamma$ for two reasons. As described above, the definition of the DPA for $\mathrm{e}^+\mathrm{e}^- \to \mathrm{WW} \to 4f + \gamma$ is non-trivial so that possible versions of DPAs should be carefully compared to the full result. Secondly, one expects a similar impact of off-shell effects, for instance induced by background diagrams, on $\mathrm{e}^+\mathrm{e}^- \to 4f + \gamma$ as in the case without photon, where such effects can reach a significant fraction of the full cross section. Therefore, they should be included at least in predictions for detectable photons, which define their own class of processes. The first full lowest-order calculation of $\mathrm{e}^+\mathrm{e}^- \to 4f + \gamma$ was performed in Ref. [36] for a definite final state, and a fully numerical treatment of all possible final states was presented in Ref. [37]. In the following we focus on the recent calculation of Ref. [16], where an event generator for all final states $4f + \gamma$ is described.

be determined from all detected final-state particles other than the muon.

$\sqrt{s}$/ GeV	200	500	1000	2000
Fixed width	82.3(3)	26.3(1)	7.29(2)	2.17(1)
Running width	82.5(3)	26.8(1)	8.29(2)	6.29(2)
Complex mass	82.0(3)	26.4(1)	7.26(2)	2.17(1)

Table 4: Cross section for $e^+e^- \to \nu_\mu\mu^+\tau^-\bar{\nu}_\tau + \gamma$ in fb for various finite-width schemes (based on the results of Ref. [16]).

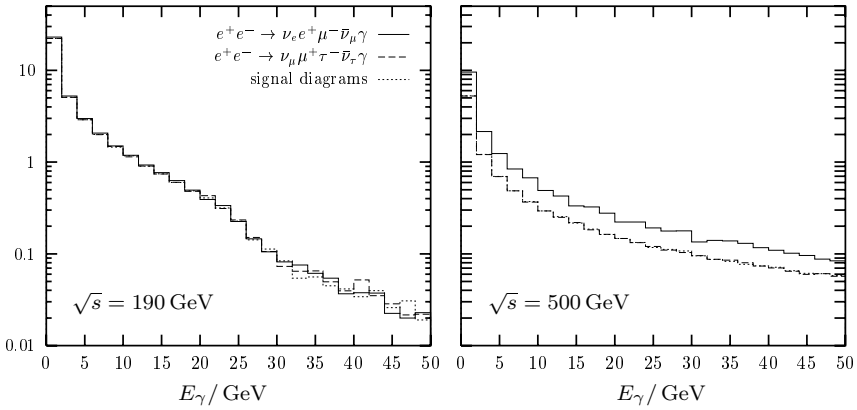

Figure 5: The photon-energy spectrum $(\mathrm{d}\sigma/\mathrm{d}E_\gamma)/(\mathrm{fb/GeV})$ of $e^+e^- \to 4f + \gamma$ for two different leptonic final states and for the approximation of including only photon emission from W-pair signal diagrams (based on the results of Ref. [16]).

In the event generator of Ref. [16] the matrix elements are constructed from simple generic functions, similar to the approach pursued in *Excalibur* [38] for $4f$ final states. Moreover, different schemes for treating gauge-boson widths are implemented, namely the ones for constant and running widths, as well as the complex-mass scheme (see Sect. 2.1). Table 4 contains some sample results on the total cross section (applying the canonical cuts of Ref. [19]) for a final state of four leptons and a photon, evaluated for LEP2 and linear-collider energies with different finite-width treatments. Similar to the case without photon emission, the SU(2)-breaking effects induced by a running width render the predictions totally wrong in the TeV range. For a constant width such effects are suppressed, as can be seen from a comparison with the results of the complex-mass scheme, which exactly preserves gauge invariance. The influence of background diagrams on predictions for $e^+e^- \to WW \to 4f+\gamma$ is illustrated in Fig. 5, where the photon-energy distribution is shown for the final states $\nu_e e^+\mu^-\bar{\nu}_\mu\gamma$ and $\nu_\mu\mu^+\tau^-\bar{\nu}_\tau\gamma$. The prediction that is based on photon emission from signal diagrams only is also included for comparison. While the impact

of background diagrams is small at the LEP2 energy of 200 GeV, there is a large background contribution already at 500 GeV for final states with $e^{\pm}$. The main effect is due to forward-scattered $e^{\pm}$, which is familiar from the results on $e^+e^- \to 4f$. More numerical results on $e^+e^- \to 4f+\gamma$ can be found in Ref. [16].

The results on $e^+e^- \to 4f + \gamma$ with detectable photons can be used as building block for four-fermion production with and without photon emission, $e^+e^- \to WW \to 4f(+\gamma)$. To this end, contributions of soft and collinear photon emission as well as virtual corrections have to be added. If a DPA is applied, care has to be taken to avoid mismatch between IR and mass singularities in virtual and real corrections. The handling of such contributions strongly depends on the details of the adopted approximations, i.e. on how the off-shellness of the W bosons is introduced, and whether background diagrams are included. Moreover, one has to make sure to avoid double-counting of real corrections when adding the non-factorizable corrections, which are described next.

3.5 Non-factorizable corrections

As already explained in Sect. 3.2, non-factorizable corrections account for the exchange of photons with $E_\gamma \lesssim \Gamma_W$ between the W-pair production and W decay subprocesses (see Figs. 2,3). Already before their explicit calculation, it was shown [39] that such corrections vanish if the invariant masses of both W bosons are integrated over. Thus, they do not influence pure angular distributions, which are of particular importance for the analysis of gauge-boson couplings. For exclusive quantities the non-factorizable corrections are non-vanishing. A first hint on their actual size was obtained by investigating the non-factorizable correction that is contained in the Coulomb singularity [40].

The explicit analytical calculation of the non-factorizable corrections was performed by different groups [41–43].[e] In these studies, the photon momentum was integrated over, resulting in a correction factor to the differential Born cross section for the process without photon emission. This correction factor is non-universal [43] in the sense that it depends on the parametrization of phase space. This is due to the problem of defining the invariant masses of the W bosons in the presence of real photon emission, which has already been described in Sect. 3.3. In Refs. [41–43] the invariant masses $M_\pm$ of the $W^\pm$ bosons are identified with the invariant masses of the corresponding final-state fermion pairs. The analytical results show that all effects from the initial e^+e^- state cancel so that the correction factor does not depend on the W-production angle and is also applicable to processes such as $\gamma\gamma \to WW \to 4f$.

[e] The original result of the older calculation [41] does not agree with the two more recent results [42, 43], which are in mutual agreement. As known from the authors of Ref. [41], their corrected results also agree with the ones of Refs. [42, 43].

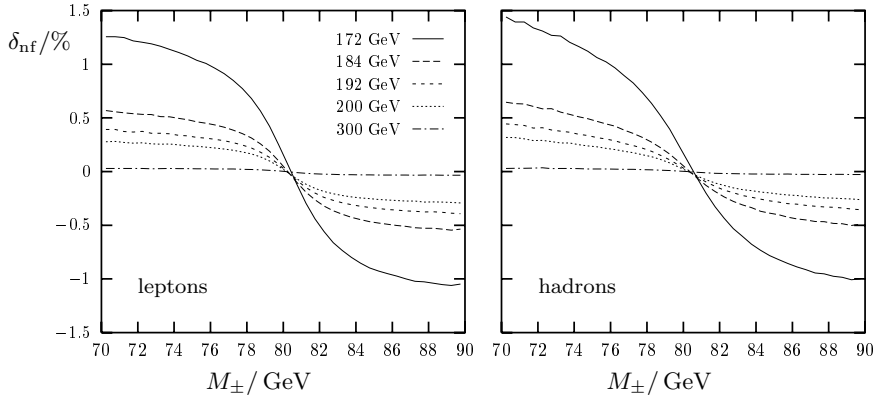

Figure 6: Relative non-factorizable corrections to single-invariant-mass distributions for $e^+e^- \to WW \to 4f$ with purely leptonic and hadronic final states (taken from Ref. [43]).

Fermion-mass singularities appear in individual contributions, but cancel in the sum of virtual and real corrections. Moreover, the correction factor vanishes like $(M_\pm^2 - M_W^2)/(\Gamma_W M_W)$ on resonance and tends to zero in the high-energy limit, both leading to a suppression of the non-factorizable corrections with respect to the factorizable ones.

The non-factorizable corrections to $e^+e^- \to WW \to 4$ leptons were numerically evaluated in Ref. [42] and for all final states in Ref. [43]. The corrections to single-invariant-mass distributions (see Fig. 6) turn out to be qualitatively similar for all final states and are of the order of $\sim 1\%$ for LEP2 energies, shifting the maximum of the distributions by 1–2 MeV, which is small with respect to LEP2 accuracy [4]. Multiple distributions in angular or energy variables and in at least one of the invariant masses of the W bosons receive larger corrections, of a few per cent.

The non-factorizable corrections to $e^+e^- \to ZZ \to 4f$ are discussed in Ref. [43], too. In this case, the corrections to the invariant-mass distributions are further suppressed and of the order of $\sim 0.1\%$, which is phenomenologically negligible. The suppression is due to an antisymmetry of the dominant parts of the differential cross sections in the angular integrations. Combined angular and invariant-mass distributions that break this antisymmetry in the integration get large corrections of several per cent. However, since the cross section for Z-pair production is, by an order of magnitude, smaller than the one for W pairs, these corrections are still not significant at LEP2.

Although non-factorizable corrections to four-fermion production turn out to be small with respect to LEP2 accuracy, they can be of relevance at future e^+e^- colliders with higher luminosity.

Acknowledgements

I would like to thank the organizers for their kind invitation and for providing a very pleasant atmosphere during the conference. F.A. Berends, A. Denner, M. Grünewald, W. Hollik, T. Riemann, M. Roth, D. Schildknecht, and D. Wackeroth are gratefully acknowledged for helpful discussions.

References

1. W. Hollik, hep-ph/9811313, plenary talk given at the *XXIXth International Conference on High Energy Physics ICHEP 98*, Vancouver, 1998.
2. H. Przysiezniak and M. Thomson, talks given at the *XXIXth International Conference on High Energy Physics ICHEP 98*, Vancouver, 1998.
3. G. Altarelli, T. Sjöstrand and F. Zwirner (eds.), *Physics at LEP2* (Report CERN 96-01, Geneva, 1996).
4. Z. Kunszt et al., in Ref. [3], Vol. 1, p. 141, hep-ph/9602352.
5. E. Accomando et al., *Phys. Rep.* **299** (1998) 1.
6. G. Gounaris et al., in Ref. [3], Vol. 1, p. 525, hep-ph/9601233.
7. W. Beenakker et al., in Ref. [3], Vol. 1, p. 79, hep-ph/9602351.
8. W. Beenakker and A. Denner, *Int. J. Mod. Phys.* **A9** (1994) 4837.
9. S. Dittmaier, *Acta Phys. Pol.* **B28** (1997) 619.
10. G. Montagna, O. Nicrosini and F. Piccinini, *Riv. Nuovo Cim.* **21** (1998) 1;
    W. Beenakker and A. Denner, *Acta Phys. Pol.* **B29** (1998) 2821.
11. A. Aeppli, G.J. van Oldenborgh and D. Wyler, *Nucl. Phys.* **B428** (1994) 126.
12. Y. Kurihara, D. Perret-Gallix and Y. Shimizu, *Phys. Lett.* **B349** (1995) 367.
13. U. Baur and D. Zeppenfeld, *Phys. Rev. Lett.* **75** (1995) 1002;
    C. G. Papadopoulos, *Phys. Lett.* **B352** (1995) 144;
    E.N. Argyres et al., *Phys. Lett.* **B358** (1995) 339.
14. W. Beenakker et al., *Nucl. Phys.* **B500** (1997) 255.
15. A. Aeppli, F. Cuypers and G.J. van Oldenborgh, *Phys. Lett.* **B314** (1993) 413.
16. A. Denner, S. Dittmaier, M. Roth and D. Wackeroth, in preparation.
17. R.G. Stuart, in Z^0 *Physics*, Proceedings of the XXVth Rencontre de Moriond, ed. J. Tran Thanh Vân, Les Arcs, 1990, p. 41.
18. G. Passarino, *Comput. Phys. Commun.* **97** (1996) 261.
19. D. Bardin et al., in Ref. [3], Vol. 2, p. 3, hep-ph/9709270.
20. A. Denner, S. Dittmaier and G. Weiglein, *Nucl. Phys.* **B440** (1995) 95;

X. Li and Y. Liao, *Phys. Lett.* **B356** (1995) 68.
21. A. Denner and S. Dittmaier, *Phys. Rev.* **D54** (1996) 4499.
22. E. Maina, R. Pittau and M. Pizzio, *Phys. Lett.* **B393** (1997) 445 and **B429** (1998) 354.
23. V.S. Fadin, V.A. Khoze and A.D. Martin, *Phys. Lett.* **B311** (1993) 311; D. Bardin, W. Beenakker and A. Denner, *Phys. Lett.* **B317** (1993) 213; V.S. Fadin et al., *Phys. Rev.* **D52** (1995) 1377.
24. M. Böhm et al., *Nucl. Phys.* **B304** (1988) 463; J. Fleischer, F. Jegerlehner and M. Zralek, *Z. Phys.* **C42** (1989) 409.
25. M. Böhm, A. Denner and S. Dittmaier, *Nucl. Phys.* **B376** (1992) 29; E: **B391** (1993) 483.
26. W. Beenakker et al., *Phys. Lett.* **B317** (1993) 622 and *Nucl. Phys.* **B410** (1993) 245.
27. S. Jadach et al., *Phys. Lett.* **B417** (1998) 326.
28. W. Beenakker, K. Kolodziej and T. Sack, *Phys. Lett.* **B258** (1991) 469; W. Beenakker, F.A. Berends and T. Sack, *Nucl. Phys.* **B367** (1991) 287; K. Kolodziej and M. Zralek, *Phys. Rev.* **D43** (1991) 3619.
29. R.G. Stuart, *Phys. Lett.* **B262** (1991) 113.
30. D.Yu. Bardin, S. Riemann and T. Riemann, *Z. Phys.* **C32** (1986) 121; F. Jegerlehner, *Z. Phys.* **C32** (1986) 425; A. Denner and T. Sack, *Z. Phys.* **C46** (1990) 653.
31. M. Kuroda, I. Kuss and D. Schildknecht, *Phys. Lett.* **B409** (1997) 405.
32. M. Kuroda and D. Schildknecht, *Nucl. Phys.* **B531** (1998) 24.
33. F.A. Berends, these proceedings.
34. W. Beenakker, F.A. Berends and A.P. Chapovsky, *Phys. Lett.* **B435** (1998) 233.
35. A. Aeppli and D. Wyler, *Phys. Lett.* **B262** (1991) 125; G.J. van Oldenborgh, P.J. Franzini and A. Borrelli, *Comput. Phys. Commun.* **83** (1994) 14; G.J. van Oldenborgh, *Nucl. Phys.* **B470** (1996) 71.
36. J. Fujimoto et al., *Nucl. Phys. (Proc. Suppl.)* **37B** (1994) 169.
37. F. Caravaglios and M. Moretti, *Z. Phys.* **C74** (1997) 291.
38. F.A. Berends, R. Kleiss and R. Pittau, *Nucl. Phys.* **B424** (1994) 308 and *Comput. Phys. Commun.* **85** (1995) 437.
39. V.S. Fadin, V.A. Khoze and A.D. Martin, *Phys. Rev.* **D49** (1994) 2247; K. Melnikov and O. Yakovlev, *Phys. Lett.* **B324** (1994) 217.
40. V.A. Khoze and W.J. Stirling, *Phys. Lett.* **B356** (1995) 373; V.A. Khoze and T. Sjöstrand, *Z. Phys.* **C70** (1996) 625.
41. K. Melnikov and O. Yakovlev, *Nucl. Phys.* **B471** (1996) 90.
42. W. Beenakker, F.A. Berends and A.P. Chapovsky, *Phys. Lett.* **B411**

(1997) 203 and *Nucl. Phys.* **B508** (1997) 17.
43. A. Denner, S. Dittmaier and M. Roth, *Nucl. Phys.* **B519** (1998) 39 and *Phys. Lett.* **B429** (1998) 145.